Calcul de l'effet Dièdre d'un Pneumatique avec des Sculptures

B. Wang et D. Duhamel
DYNAMIQUE, LABO NAVIER, ENPC, Cité Descartes, 6-8 Avenue Blaise Pascal, 77455 Champs-Sur-Marne, France
bin.wang@enpc.fr

This paper proposes a method to compute the horn effect for tire with treads. The main feature of the method is that it can easily get the sound pressure around the horn-like structure which has grooves with small cross sections on the surfaces. It greatly saves computational costs and gives more physical informations. It is based on the boundary element method, and divides the computational domain of horn effect into an exterior subdomain of tire and several interior subdomains of junctions. It needs BEM system matrices and excitation vector, and also the relation of pressure and velocity between the subdomains ends which can be obtained by analytical or numerical methods. This method is applied to study some simple examples for which analytical or numerical results are available. Good agreements between the proposed method and known results can check its efficiency and accuracy. Then horn effect of tires with treads is computed by this method, and comparisons with smooth tires are made.

1 Introduction

Between the tire and road, there is a horn-like geometry formed by the surfaces of tire and road. It greatly amplifies the sound pressure for sound sources. According to the experimental measurements in [1], the horn effect is responsible for about 10-20dB increase in noise level. Numerical calculations using the indirect boundary element method (BEM) have been carried out by Graf as well. The BEM results agree well with experiment below 2500 Hz. However, the BEM results don't give a physical explanation for the frequency dependence of the horn amplification. Then Graf used asymptotic theories to describe the horn effect at low and high frequencies. Good quantitative predictions and the physical aspects of the phenomenon were given. In [2] the sound pressure and sound amplification of horn effect are calculated in the space around the 3D tire model using the BEM. The influence of different parameters such as the position and size of the source are studied. It is shown that the position of the source has a very important influence, while its size has negligible influence. The influence of roads' absorption properties on the amplification is also analyzed.

However, the tire in the previous numerical calculations is represented as a short cylinder with smooth surfaces. Actually there are treads around the tire surface which should be taken into account. For the tire with complicated treads, it is difficult to get the sound pressure near the tire which is essential to the computation of horn effect. Tire with treads can be considered as flanged waveguides. In such systems, the waveguides are formed by the road and tire in the contact zone and have small cross sections. The BEM is available, but only for very simple case as BEM needs fine mesh around the resonant frequency of the waveguide to get converged solutions. For complicated waveguide, fine mesh leads to high computational costs, so new methods should be used. Since the cross sections of waveguides are neither as small as the arbitrary microscopic holes in many porous materials nor as big or complicated as the pipes in the mufflers, it is not suitable to use the same methods to calculate the sound pressure field of the flanged waveguide. But the methods for mufflers could give some inspirations. Mufflers have complicated internal structures. There are several methods for the analysis of mufflers summarized in [3]. The multi-domain BEM and BEM with the transfer matrix could be used for the calculation of the flanged waveguide, but some changes should be made.

A brief introduction of the applications of multi-domain BEM can be seen in [4]. It was first used to analyze the potential problem and elasticity [5]. Then it was introduced to solve acoustic problems. An important application of multi-domain BEM to acoustics is the coupled interior/exterior problems [6]. The multi-domain BEM is also used to deal with problems with several acoustic media [7]. Another wide application is the problem about thin bodies [8] before using the hypersingular integral equation. Dividing the whole acoustic domain into several subdomains is the main idea of the multi–domain BEM. Substructuring can reduce the matrix size and the total computational time for large structures, but the adjacent subdomains should have the same interface mesh to match the boundary conditions.

Transfer matrix techniques have been applied to the analysis of series of connected pipes with many changes of sectional area in [9]. In [10] a different form of transfer matrix is used, together with the matrices derived for the two-dimensional junctions by finite element method, to describe a complete network. In [11] the transfer matrix is used to combine the impedance matrix of each substructure of a silencer. The transfer matrix can easily connect two substructures and describe the relation of pressure and particle velocity between them. But an assumption should be true to get the transfer matrix, which is the plane wave propagation in the connected part.

Since BEM is advantageous for analyzing problems with an exterior domain or a complex geometry, in this paper a substructuring technique based on BEM is proposed to reduce matrix size of the strcture, and also a modified transfer matrix is used to connect the subdomains to reduce the nodes and elements and avoid the identical mesh at the interface.

First the structure to be analyzed and wave propagation are introduced. The computational method is described in the next section. Then comparisons are given to check the accuracy of the proposed method. Finally tire with treads is solved with the proposed method.

2 Problem specification

To compute the amplification of horn effect, the sound pressure around the tire and road should be obtained first. Tire with treads can be treated as flanged waveguides. The surfaces of tire and road are the flanges, and the tire treads and road form the waveguides which could have any connection pattern : arbitrary network, parallel pipes or a mixture of them. The waveguides in this paper have small cross sections.

2.1 Wave propagation

Fig.1a represents three dimensional network with arbitrary flange. Put a point source S near the flange. The acoustic wave at point R includes three parts (see Fig.1a) : wave directly from the source, wave reflected from the

flanged without network (see Fig.1b) and wave radiating from the network with flange (see Fig.1c). The wave from the source arrives at pipes ends and then propagates in the network. The straight parts of the network are very thin compared with the wave length to be analyzed. So there is only plane wave motion in the straight parts. The wave in the junction of the network has higher order modes, but it doesn't propagate in the straight parts. In Fig.1b, we use imaginary pipes ends instead of the real ends. The imaginary ends are inside the network but close to the real ones. The imaginary surfaces S_{imag} are perpendicular to pipes walls. Thus, at S_{imag} the wave is uniform, which is useful in the method proposed in this paper. However, it is not uniform at the real ends, even if the real ends are perpendicular to the network walls, because the cross sections change suddenly.

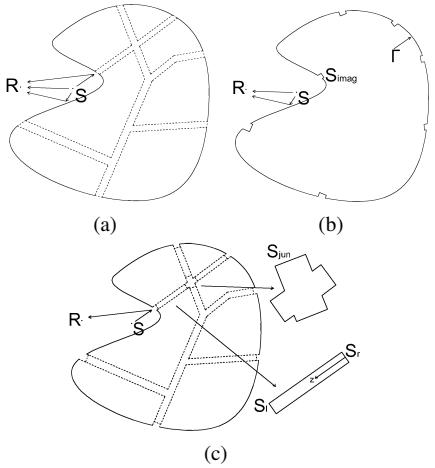

FIGURE 1 – (a) Total pressure ; (b) Pressure directly from source and reflected by flange ; (c) Pressure radiating from network

2.2 Boundary condition

The boundary condition of flange and waveguide walls could be the pressure, the normal derivative of the pressure, the impedance, the surface velocity, or a mixture of them. There should be a small transition zone between different boundary conditions.

3 Computational method

The calculation of the total acoustic pressure p_{tot} at a point R in the exterior domain in Fig.1a is the first step of the computation of horn effect.

3.1 The total pressure

The waveguide to be analyzed consists of cylindrical or rectangular pipes with small cross sections. For very simple waveguides one can get the total pressure easily by running BEM once. However, around the resonant frequency of the waveguide it needs fine mesh to get converged results by BEM. So the computational costs are very high. For complicated networks, fine mesh leads to memory problem of computer. To avoid this problem, a multi-domain BEM combined with transfer matrix technique is proposed.

In boundary element methods, for a problem with a bounded domain, the integral equation to be solved is given by

$$c_e(\mathbf{x})p(\mathbf{x}) = \int_\Gamma p(\mathbf{y})\frac{\partial G}{\partial \mathbf{n}_y}(\mathbf{x},\mathbf{y})d\mathbf{y} - \int_\Gamma \frac{\partial p}{\partial \mathbf{n}_y}(\mathbf{y})G(\mathbf{x},\mathbf{y})d\mathbf{y} + p_{inc}(\mathbf{x}) \quad (1)$$

Γ is the surface of a bounded domain. $p_{inc}(\mathbf{x})$ is the incident pressure from the source without the structure. G is the Green function. $\mathbf{n}$ is the unit normal vector pointing into the domain. To get the total pressure p_{tot} in the exterior domain, let $c_e(x) = 1$. Γ includes the flange and the imaginary network ends (see Fig.1b). Substitute pressure $p(\mathbf{y})$ and its derivative $\frac{\partial p}{\partial \mathbf{n}_y}$ on the surface Γ into Eq. (1) and solve it, one has p_{tot}. These values should be calculated first.

3.2 Unknowns on surface Γ

Divide the problem in Fig.1a into an exterior subdomain of flange and several interior subdomains of junctions. Solve each subdomain by BEM to get BEM system matrices and excitation vector, and then connect the subdomains by transfer matrices. Finally solve the overall equation system, and one has $p(\mathbf{y})$ and $\frac{\partial p}{\partial \mathbf{n}_y}$ on surface Γ. The process is described in detail in the following.

3.2.1 Subdomains

In Eq. (1), for a point $\mathbf{x}$ on Γ, $c_e(\mathbf{x})$ equals 1/2 if the surface Γ is regular at this point. The discretization of Eq. (1) is obtained from a mesh of the surface of the domain. Then a linear system (2) can be obtained whose solution gives an approximation of the solution on the surface Γ. More information can be found in [12].

$$\mathbf{AP} + \mathbf{BQ} = \mathbf{P}_{inc} \quad (2)$$

$\mathbf{P}$, $\mathbf{Q}$ and $\mathbf{P}_{inc}$ are vectors of pressure, derivative of pressure and incident pressure, respectively. $\mathbf{A}$ and $\mathbf{B}$ are BEM system matrices.

For the exterior subdomain in Fig.1b, divide the vectors in Eq. (2) into vectors of imaginary ends and vectors of flange. One has

$$\mathbf{A}_E \begin{bmatrix} \mathbf{P}_{ep} \\ \mathbf{P}_f \end{bmatrix} + \mathbf{B}_E \begin{bmatrix} \mathbf{Q}_{ep} \\ \mathbf{Q}_f \end{bmatrix} = \begin{bmatrix} \mathbf{P}^{ep}_{inc} \\ \mathbf{P}^{f}_{inc} \end{bmatrix} \quad (3)$$

The subscripts and superscripts ep and f mean the imaginary ends of straight pipes and the flange, respectively. Matrices $\mathbf{A}_E$ and $\mathbf{B}_E$ can be obtained by solving the problem in Fig.1b with BEM software. In the BEM software, using the rigid boundary condition on the surface Γ, one can get $\mathbf{A}_E$. Using the soft boundary condition, one can get $\mathbf{B}_E$. The incident pressure p_{inc} can be obtained in either of the two computations above.

For the network in Fig.1c we create imaginary surfaces for its junctions. These surfaces should be perpendicular to the network walls. One can see the interior subdomain of a junction in Fig.1c. The normal direction of surface S_{jun} points inward. Since for the junction subdomain there is no source, the incident pressure equals zero. The equations system for the junction is

$$\mathbf{A}_I \begin{bmatrix} \mathbf{P}_{ej} \\ \mathbf{P}_w \end{bmatrix} + \mathbf{B}_I \begin{bmatrix} \mathbf{Q}_{ej} \\ \mathbf{Q}_w \end{bmatrix} = \begin{bmatrix} \mathbf{0} \\ \mathbf{0} \end{bmatrix} \tag{4}$$

The subscripts and superscripts ej and w mean the imaginary ends and the walls of junction. Matrices $\mathbf{A}_I$ and $\mathbf{B}_I$ can be obtained by running the BEM software in the same way as before.

3.2.2 Transfer matrix

The straight pipe between the flange and the junction or two junctions in Fig.1c, whose central axis is labelled as z, is thin compared to the wavelength to be analyzed. There is only plane wave. Pressure p and its derivative q are constant on a plane perpendicular to z. The wave equation is

$$\frac{\partial^2 p}{\partial z^2} = \frac{1}{c^2}\frac{\partial^2 p}{\partial t^2} \tag{5}$$

c is the sound speed. Suppose that the solution of Eq. (5) is

$$p(z) = a\cos kz + b\sin kz \tag{6}$$

k is the wave number. The convention $e^{-i\omega t}$ is adopted, where $i^2 = -1$, ρ is the density of air and ω is the angular frequency. The velocity is given as

$$v(z) = \frac{1}{i\rho\omega}\frac{\partial p}{\partial z} \tag{7}$$

Surfaces S_r and S_l in Fig.1c have different normal directions. Substitute $z = z_r$ and $z = z_l$ into Eqs. (6) and (7), then one can get the relation of p and q between one node on S_r and another node on S_l. Since p can be expressed as the mean value because the pressure is constant at each pipe end, q at any node i on S_r and S_l becomes

$$\begin{bmatrix} q_{ri} \\ q_{li} \end{bmatrix} = \begin{bmatrix} t_{11} & t_{12} \\ t_{21} & t_{22} \end{bmatrix} \begin{bmatrix} \dfrac{1}{n_r}\displaystyle\sum_{j=1}^{j=n_r} p_{rj} \\ \dfrac{1}{n_l}\displaystyle\sum_{j=1}^{j=n_l} p_{lj} \end{bmatrix} \tag{8}$$

Here n_r and n_l are node numbers at each end. Thus, the relation between p vector $\mathbf{P}_e$ and q vector $\mathbf{Q}_e$ at the two ends can be written as

$$\mathbf{Q}_e = \mathbf{S}\mathbf{P}_e \tag{9}$$

3.2.3 Solving simultaneous equations

For the whole problem of flanged waveguide in Fig.1a, one has the Eqs. (3), (4) and (9) of each couple of ends, so the overall system can be assembled. After applying the boundary condition in section 2.2 to the flange and tube walls and solving the overall system, the values of p and q for each node on the surfaces Γ and S_{jun} can be obtained.

4 Comparison with known solutions

For simple waveguides and flanges, there are analytical solutions and the BEM works. We calculate the pressure at imaginary ends of the waveguide and the total pressure at a point outside the flange and then compare with the method proposed to check its accuracy. The first example is a straight pipe. The seconde one is a T pipe.

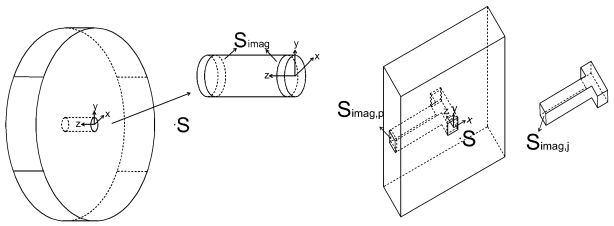

FIGURE 2 – (a) One pipe with cylindrical flange ; (b) T pipe with rectangular flange.

4.1 Straight pipe

The flange in this example is a cylinder. There is a thin pipe at the center (see Fig.2a). The flange and pipe wall are rigid. The radius of the pipe and the flange is $0.005m$ and $0.6m$ respectively. The pipe length is $0.1m$. The source S is at $(0, 0, -0.1)$. We create imaginary ends for the pipe to ensure that the pressure is uniform at these ends. The coordinates of the imaginary ends are $z = 0.005$ and $z = 0.095$ (see Fig.2a).

4.1.1 Analytical method

The total pressure can be calculated by

$$p_{tot} = p_{rad} + p_{inc} \tag{10}$$

p_{inc} in this part is the incident pressure at point R $(0.1, 0.1, -0.1)$ from the source and reflected by the flange without waveguide. p_{rad} is the pressure radiating from the waveguide.

The first step to get p_{rad} is calculating the pressure p_{end} and particle velocity v_{end} at the imaginary ends analytically. Since the pipe is straight and thin, there is only plane wave. One has Eq. (5) and its solution Eqs. (6) and (7). Substitute $z = 0$ and $z = l$ into them, one gets the expressions of pressure p_{rt}, p_{lt} and velocity v_{rt}, v_{lt} at the real ends of the pipe. At the two real ends the pressure and velocity include two parts : radiating part and incident part. Substitute them into the expressions of pressure and velocity obtained before, one has

$$p_{rr}\cos kl + i\rho c v_{rr}\sin kl - p_{lr} = -p_{ri}\cos kl - i\rho c v_{ri}\sin kl + p_{li} \tag{11}$$

$$p_{rr}\sin kl - i\rho c v_{rr}\cos kl + i\rho c v_{lr} = -p_{ri}\sin kl + i\rho c v_{ri}\cos kl - i\rho c v_{li} \tag{12}$$

p_{rr} and v_{rr} are values of wave radiating from the right real end, and p_{lr} and v_{lr} are from the left real end. p_{ri} and v_{ri} are values of incident wave at the right real end, and p_{li} and v_{li} are at the left real end. The pressure and velocity radiating from the pipe satisfy

$$\frac{p_{rr}}{v_{rr}} = -Z_r \tag{13}$$

$$\frac{p_{lr}}{v_{lr}} = Z_r \tag{14}$$

Z_r is the radiation impedance. Since the flange is big compared to the pipe and the source is close to the pipe, the flange can be considered as infinite. One has $Z_r = \rho c(\frac{1}{2}(kr)^2 - i(0.8216kr))$, where r is the pipe radius.

From Eqs. (11)-(14) one can obtain a system of linear equations. In this system, p_{ri}, v_{ri}, p_{li} and v_{li} should be given. In Fig.2a if we close the real ends of the pipe and then put rigid boundary condition on the whole surface, these values can be obtained by BEM, and so is the incident pressure p_{inc} at receiver R in the exterior domain. After substituting them into the system and solving, one can get the pressures p_{rr}, p_{lr} and velocities v_{rr}, v_{lr} at the two ends for a given frequency.

Then one can get a and b from the expressions of pressure and velocity. Substitute them in Eq. (6), one obtains the pressure p_{end} and v_{end} at the imaginary ends. With p_{end}, the pressure p_{rad} radiating for the pipe can be obtained by BEM. Closing the pipe at imaginary ends in Fig.2a, putting p_{end} on the end surfaces and rigid boundary condition on the other part of surface, removing the source, and solving this problem by BEM, one has p_{rad} at R. Then the total pressure at the point R can be obtained by Eq. (10).

4.1.2 Comparison

One can solve this problem by the multi-domain BEM (M-BEM) introduced in section 3. There is no junction, so only the Eqs. (3) and (9) are needed.

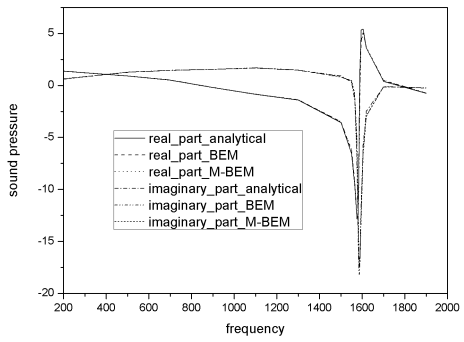

FIGURE 3 – Pressure at right imaginary end of straight pipe

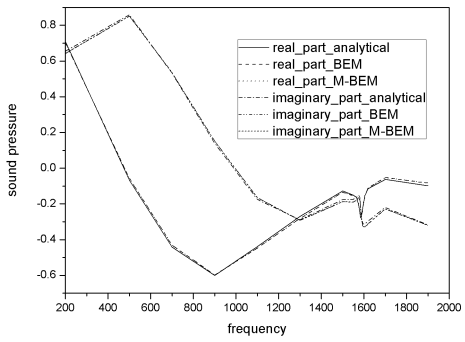

FIGURE 4 – Pressure at point R near flange

Fig.3 and 4 are the pressures at the right imaginary end of the straight pipe and at point $R(0.1, 0.1, -0.1)$ calculated by three methods. Good agreement can be seen in these figures. The error of pressure between two different methods can be calculated by $error = |p_1 - p_2|/|p_1|$. At point R, the maximum error between M-BEM and BEM is 2.6%, and the maximum error between M-BEM and analytical method is 7.5%. In the analytical method, the assumption of uniform pressure at the real pipe ends is used. Actually it is not plane wave at the real ends, for the pipe radius changes suddenly. This assumption brings error. Its influence on pressure in the exterior domain is smaller than at the imaginary ends.

4.2 T pipe

The flange in this example is a hexahedron. There is a T pipe at the center (see Fig.2b). The flange and pipe wall are rigid. The cross section of the pipe and the flange is $0.02 \times 0.02m$ and $0.3 \times 0.3m$ respectively. The pipe length is $0.1m$ and the branch length is $0.14m$. The source S is at $(0, 0, -0.1)$. We create imaginary ends $S_{imag,p}$ for the T pipe to ensure that the pressure is uniform at these ends. The distance between imaginary ends and real ends is $0.005m$(see Fig.2b). Then we create imaginary surfaces $S_{imag,j}$ for the junction. The distance between $S_{imag,p}$ and $S_{imag,j}$ is $0.005m$.

In multi-domain BEM, assemble and solve Eqs. (3), (4) and (9) of each couple of imaginary surfaces $S_{imag,p}$ and $S_{imag,j}$, one can get the solution. By Eq. (1) one has the sound pressure field. Fig.5 and Fig. 6 are the pressures at the imaginary end ($z = 0.005m$) and at point $R(-0.1, 0.1, -0.1)$ calculated by two methods. In Fig.6 there is good agreement. The maximum error of pressure at point R between M-BEM and BEM is 1.4%.

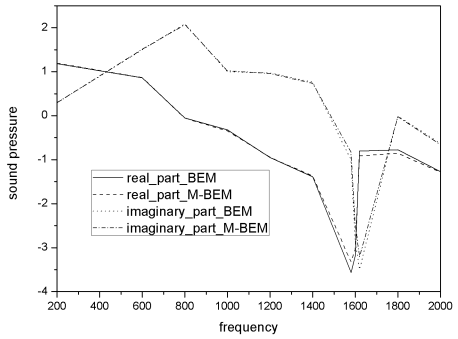

FIGURE 5 – Pressure at the imaginary end of straight pipe

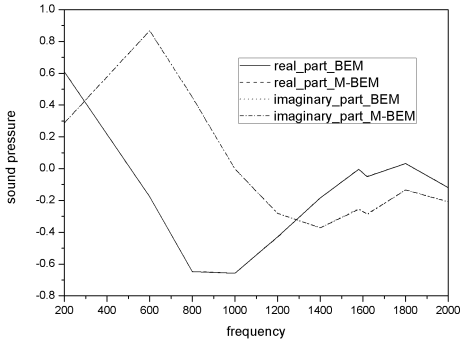

FIGURE 6 – Pressure at point R near flange

In Fig.5, one can see good agreement between these two methods as well. There are small differences around the resonant frequency which is about $1600Hz$. The reason may be that the assumption of plane wave in M-BEM is not perfect for this rectangular cross section pipe around $1600Hz$.

5 Horn effect of tire with treads

The sound pressure P around a horn-like structure between tire and road can be computed with the proposed method. Then it is easy to get the amplification of horn effect with the following formula.

$$A = 20log(\frac{P}{P_{ref}}) \quad (15)$$

P_{ref} is the sound pressure without road.

In this section, the amplification of horn effect for a tire with treads is computed and compared with smooth tire. The tire in Fig.7a is flat in the contact zone. The road and tire is rigid. There are three grooves around the tire and one transversal groove. The cross section of the grooves is $0.005 \times 0.005m$ except the circular groove in the middle which has the cross section $0.005 \times 0.01m$. The radius and width of tire are $0.27m$ and $0.15m$, respectively. The contact zone is $0.1m$ in length. The source S is at $(0.1, 0, 0.005)$, and the receiver R is at $(1, 0, 0.265)$. $S2 - S6$ are the surfaces of network ends. Fig.8 is the mesh of tire with treads, and it is used to compute the pressure P_{ref} around tire without road.

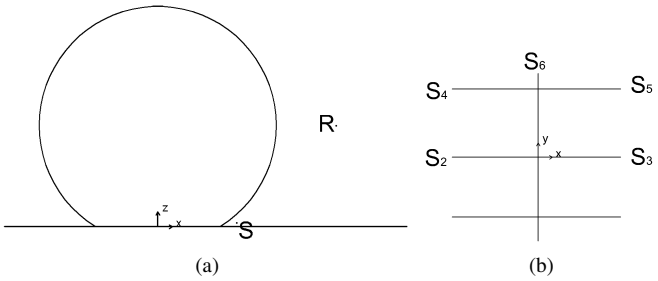

FIGURE 7 – (a) Horn-like structure between tire and road ; (b) Network in the contact zone

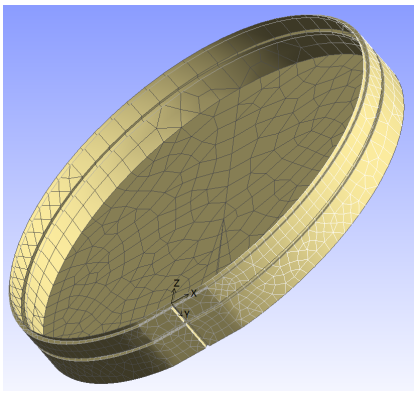

FIGURE 8 – Half of a tire with treads

Fig.9 shows the pressure at network ends. We can see peaks around $1250Hz$, and it is due to the air resonance in the network. So in Fig.10 there are big differences of amplification of horn effect between the tire with treads and smooth tire around this frequency. Therefore, the treads should be taken into account in the computation of horn effect.

6 Conclusion

The multi-domain BEM proposed in this paper makes it possible to calculate the horn effect of tire with treads.

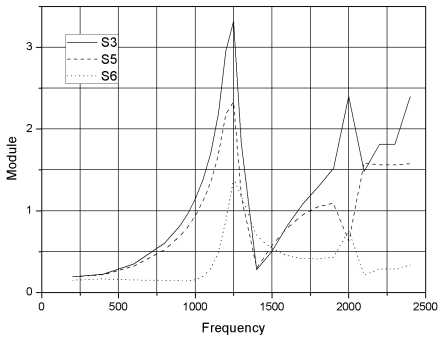

FIGURE 9 – Pressure at network ends

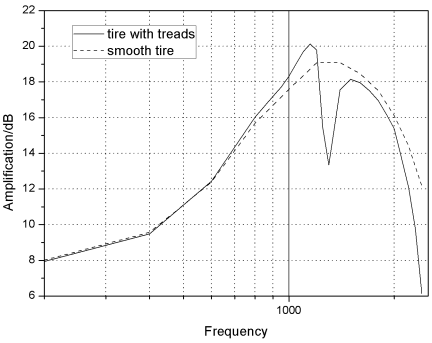

FIGURE 10 – Comparison of amplification of horn effect

It uses substructuring and transfer matrix techniques to reduce nodes, elements and the BEM matrix size and to save computational memory. Only the tire surfaces and network junctions need to be modeled. It combines the advantages of boundary element method and transfer matrix technique together. The method has good accuracy. The influences of treads on the horn effect of tire/road are big, and the optimizations of treads should be done in the future to reduce the amplification of horn effect.

Références

[1] R. Graf, C.-Y. Kuo, A. Dowling, W. Graham, On the horn effect of a tyre/road interface, part i : Experiment and computation, Journal of Sound and Vibration 256 (3) (2002) 417–431.

[2] A. Fadavi, Modélisation numérique des vibrations d'un pneumatique et de la propagation du bruit de contact, Ph.D. thesis, Ecole Nationale des Ponts et Chaussées (2002).

[3] Y.-B. Park, H.-D. Ju, S.-B. Lee, Transmission loss estimation of three-dimensional silencers by system graph approach using multi-domain bem, Journal of Sound and Vibration 328 (4) (2009) 575–585.

[4] T.-W. Wu, Multi–domain boundary element method in acoustics, in : Computational Acoustics of Noise Propagation in Fluids-Finite and Boundary Element Methods, Springer, 2008, pp. 367–386.

[5] C. Brebbia, S. Walker, Boundary Element Techniques in Engineering, Newnes-Butterworths, 1980.

[6] C. R. Cheng, Boundary Element Analysis of Single and Multidomain Problems in Acoustics, Ph.D. thesis, UNIVERSITY OF KENTUCKY. (1988).

[7] H. Utsuno, T. W. Wu, A. F. Seybert, T. Tanaka, Prediction of sound fields in cavities with sound absorbing materials, AIAA Journal 28 (1990) 1870–1876.

[8] C. Cheng, A. Seybert, T. Wu, A multidomain boundary element solution for silencer and muffler performance prediction, Journal of Sound and Vibration 151 (1) (1991) 119–129.

[9] M. L. Munjal, M. Munjal, Acoustics of ducts and mufflers with application to exhaust and ventilation system design, Wiley New York (NY) et al., 1987.

[10] A. Craggs, D. Stredulinsky, Analysis of acoustic wave transmission in a piping network, The Journal of the Acoustical Society of America 88 (1990) 542.

[11] G. Lou, T. Wu, C. Cheng, Boundary element analysis of packed silencers with a substructuring technique, Engineering Analysis with Boundary Elements 27 (7) (2003) 643–653.

[12] D. Duhamel, L'acoustique des problèmes couples fluide-structure-application au contrôle actif du son, Ph.D. thesis, Ecole des Ponts ParisTech (1994).